applied optics

Customized retarders based on waveplates

JOSE LUIS VILAS* AND JOSE MARIA HERRERA-FERNANDEZ

Information Technology Department, Escuela Politécnica Superior, Universidad San Pablo-CEU, CEU Universities, Urbanización Montepríncipe, 28668 Boadilla del Monte, Madrid, Spain
**Corresponding author: jlvilas@cnb.csic.es*

Received 16 June 2022; revised 16 August 2022; accepted 21 August 2022; posted 22 August 2022; published 8 September 2022

Phase control is a critical parameter in polarization measurements. It is well known that a proper combination of wave plates allows to obtain achromatic phase shift, i.e., a constant retardation in certain spectral ranges. This paper is focused on a different, but more useful, goal, as it is to achieve customized variable retarders in broad spectral ranges. To do that, a merit function was used to measure the similarity between the overall phase shift of the wave plate combinations and the desired target. The control variables are the thicknesses and orientations of the wave plates. All possible combinations with four and five wave plates of quartz and MgF_2 were analyzed, but our approach can be perfectly extended to deal with more wave plates. The result of an optimization process determines the thicknesses and orientations of the wave plates, which results in the closest retarder to the desired one. Numerical results show deviations below 10% between the target and the obtained retardation. These systems are of special interest in those fields and instruments in which polarization control plays a fundamental role.

https://doi.org/10.1364/AO.468065

1. INTRODUCTION

The polarization of the light is a physical phenomenon with numerous applications in polarimetry, optical communications systems, nanophotonics, and spectroscopy, among many others [1–5]. Different methods and optical configurations have been used to obtain light beams with specific polarization properties; some examples are Fresnel rhombs [6], birefringence wave plates [7], and linear polarizers [3]. If we are focused on the obtainment of achromatic systems through wave plates, one of the most famous techniques is the well-known Pancharatnam method. It considers a system composed of three wave plates, and attempts to determine the orientations of the wave plates to achive an achromatic retarder [7]. Originally, the material was the same for all involved wave plates. However, Hariharan proposed a modified method where two wave plates with specific thicknesses and different materials are used [8,9]. Since then, several techniques have been proposed to increase the achromatic behavior of these systems. For instance, it is possible to use subwavelength diffraction gratings where the grating acts as an optically anisotropic medium [10,11]. Other options are a combination of twisted nematic liquid-crystal cells considering material dispersion [12], the use of stacks of thin films [13], or complex structures inspired by animals [14]. Nevertheless, an easier way is to provide more degrees of freedom in the Hariharan system by increasing the number of wave plates placed in cascade. In this sense, six quartz wave plates were used in the achromatic system proposed by Mason, [15] where the parameters of each plate are optimized in the terahertz spectrum. In this spectral range, Ma optimized systems with three, six, and 10 layers with the simulated annealing algorithm [16]. Following the same idea, Chen used a merit function that incorporates the optical axis and output linearity to optimize an achromatic system of nine wave plates [17]. In the case of the visible range, the use of commercial wave plates is common. Nevertheless, this limits the optimization of the system [18–20]. Variations of the Hariharan method to design achromatic retarders in the visible spectrum were recently proposed, suggesting an analytical method to define the achromatic retarder [21]. Unfortunately, this analytical method considers the fast axis of all wave plates parallel each other; if this constraint is released, the calculation of the overall retardation can be quite complex, or even lack a close form. In those cases, it is necessary to make use of computational techniques, such as the one proposed in [22], which is a superachromatic quarter-wave retarder using an arbitrary number of wave plates in a broadband spectral range. In that work, the optimization of thicknesses and azimuths is achieved using a merit function known as achromatism degree (AcD). The study is focused on two spectral ranges, 500–700 nm and 400–1000 nm, being the maximum difference with respect to the target retardation, 0.013° and 0.010°, respectively. However, this method is limited to the case where the target retardation is constant at any wavelength.

In this work, we analyze the feasibility for obtaining free-shaped retarders by combining four or five wave plates of quartz and MgF_2. There are 32 possible combinations of these two kinds of materials. All of these combinations are explored by searching the thicknesses and the orientations of each wave plate

to achieve specific target retardation. The combinatorial nature of this problem and the two variables per wave plate (orientation and thickness) imply that the problem presents a deep computational effort. The computational burden is even more complicated taking into account the complex dependence of the refractive index on wavelength. The target retarder is achieved by means of optimization of the AcD [23], where the control variables are thicknesses and azimuths. We assume that the wave plates are transparent media arranged in cascade.

2. THEORETICAL ANALYSIS

Consider the scheme shown in Fig. 1 where a set of N wave plates perfectly aligned is disposed parallel to each other in a cascade configuration. A beam with spectrum $g(\lambda)$ lights the system orthogonally to each wave plate.

The system is modeled by means of the Jones formalism, in which each wave plate is described by a matrix 2×2 complex matrix, C_j. From this point, any subscript j of a matrix or variable will make reference to the position of the retarder. For instance, C_j denotes the Jones matrix of the retarder located in position j of the system given by

$$C_j(\phi_j, \delta_j) = \begin{pmatrix} \cos\frac{\delta_j}{2} + i\,\sin\frac{\delta_j}{2}\cos 2\phi_j & i\,\sin\frac{\delta_j}{2}\sin 2\phi_j \\ i\,\sin\frac{\delta_j}{2}\sin 2\phi_j & \cos\frac{\delta_j}{2} - i\,\sin\frac{\delta_j}{2}\cos 2\phi_j \end{pmatrix}, \tag{1}$$

where i is the imaginary unit, and δ_j, ϕ_j are the retardation and azimuth of the fast axis, respectively, both belonging to the wave plate in position j. Without loss of generality, the origin of angles can be fixed as the fast axis of the first wave plate, i.e., $\phi_1 = 0$, ϕ_j being the angle between the fast axis of the first wave plate and the retarder located at position j. The retardation, δ_j, contains information about the material of the wave plate and shows the following dependence on wavelength:

$$\delta_j = \frac{2\pi\,\Delta n_j(\lambda)}{\lambda}\,d_j, \tag{2}$$

where d_j is the thickness of the wave plate and $\Delta n_j(\lambda)$ the birefringence at the wavelength, λ. The birefringence is defined as the difference between the ordinary refractive index, n_o, and extraordinary, n_e, associated with the fast and slow axes of the wave plate, respectively. The exact dependence of n_o and n_e on λ is usually given via experimental Sellmeier relations [24]. As a consequence, the retardation presents a complex dependence on wavelength. The polarimetric behavior for the whole configuration with N wave plates is given by the matrix product, M, of all wave plates, C_j:

$$M = \prod_{j}^{N} \mathbf{C}_j(\phi_j, \delta_j). \tag{3}$$

Due to $\mathbf{C}_j(\phi_j, \delta_j) \in \mathrm{SU}(2)$, the product, $M \in \mathrm{SU}(2)$, and therefore M, can be written as

$$M = \begin{pmatrix} A & B \\ -B^* & A^* \end{pmatrix}. \tag{4}$$

Note that the proposed model considers that all energy of the beam of light is conserved, neglecting the transmittance of the wave plates. This model should be accurate enough, but more refined models including the transmittance of wave plates can also be considered. The Jones equivalence theorem establishes that a configuration composed of an arbitrary number of retarders is equivalent to a single retarder and a rotator [25]. The reader can find a modern approach to prove this theorem in [26]. In mathematical terms, this equivalence is expressed as

$$M = R(\omega)\,C(\Psi, \Delta), \tag{5}$$

where $R(\omega)$ is the rotator matrix with rotation angle ω:

$$R(\omega) = \begin{pmatrix} \cos\omega & -\sin\omega \\ \sin\omega & \cos\omega \end{pmatrix}, \tag{6}$$

$$C(\Psi, \Delta) = \begin{pmatrix} \cos\frac{\Delta}{2} + i\,\sin\frac{\Delta}{2}\cos 2\Psi & i\,\sin\frac{\Delta}{2}\sin 2\Psi \\ i\,\sin\frac{\Delta}{2}\sin 2\Psi & \cos\frac{\Delta}{2} - i\,\sin\frac{\Delta}{2}\cos 2\Psi \end{pmatrix}, \tag{7}$$

is the retarder matrix with overall retardation Δ and azimuth Ψ, and therefore

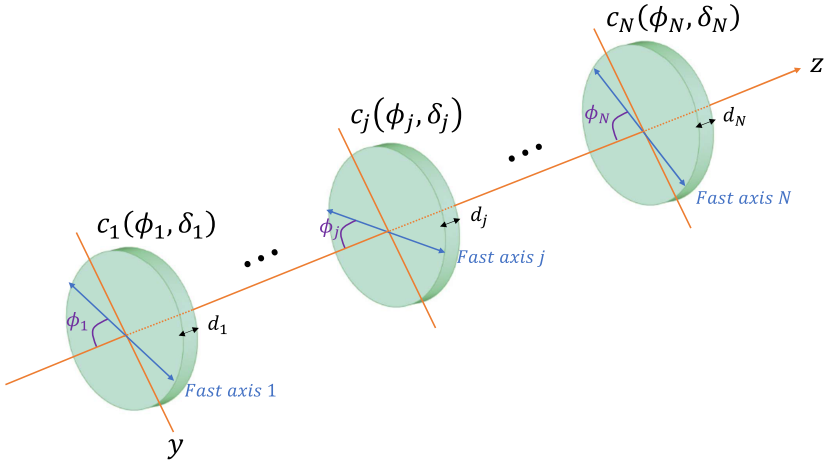

Fig. 1. Scheme of the configuration composed by N wave plates in cascade. $\mathbf{C}_j(\phi_j, \delta_j)$ is the matrix of the jth wave plate, where ϕ_j is the azimuth, δ_j is the retardation, and d_j is the thickness.

$$A = \cos\omega\cos\frac{\Delta}{2} + i\left[\cos\omega\sin\frac{\Delta}{2}\cos 2\Psi - \sin\omega\sin\frac{\Delta}{2}\sin 2\Psi\right], \quad (8)$$

$$B = -\sin\omega\cos\frac{\Delta}{2} + i\left[\sin\omega\sin\frac{\Delta}{2}\sin 2\Psi + \cos\omega\sin\frac{\Delta}{2}\cos 2\Psi\right] \quad (9)$$

are the components of M. It allows to obtain the overall retardation as

$$\tan^2\left(\frac{\Delta}{2}\right) = \frac{|\mathrm{Im}(A)|^2 + |\mathrm{Im}(B)|^2}{|\mathrm{Re}(A)|^2 + |\mathrm{Re}(B)|^2}, \quad (10)$$

where $\mathrm{Re}(X)$ and $\mathrm{Im}(X)$ denote the real and the imaginary parts of the complex number X, respectively. Parameters A and B depend on the wavelength; therefore, the overall retardation will also be complex. The chromatic behavior of an optical element in a spectral range can be characterized by the merit function called AcD [22,23]. This metric consists of a measurement of the distance between the overall retardation and the target retardation, Δ_0, weighted by the light spectrum, $g(\lambda)$, in a spectral range, $\Omega = [\lambda_{\min},\ \lambda_{\max}]$:

$$\mathrm{AcD} = \frac{\sqrt{\int_\Omega |\Delta(\lambda) - \Delta_0(\lambda)|^2 g(\lambda)\,\mathrm{d}\lambda}}{\sqrt{\int_\Omega g(\lambda)\,\mathrm{d}\lambda}}. \quad (11)$$

Note that the spectrum acts as a weight function. In this work, the AcD metric is used for defining customizable/free-shaped retarders in the spectral region $\Omega = [500,\ 700]$ nm; however, it is perfectly extrapolated to other spectral ranges. The target retardation, $\Delta_0(\lambda)$, is a chosen function that presents a specific shape defined by a designer, for instance, a step function. The objective is then to fit the overall retardation given by Eq. (10) to the target retardation, $\Delta_0(\lambda)$. The parameters that allow to control the fitting are the N thicknesses and $N-1$ azimuths of the wave plates. The fitting can be performed by minimizing the AcD metric by means of the $2N-1$ variables, and defining the optimization problem. The Lagarias method was used as the algorithm to solve this optimization problem [27].

Other important design parameters are the materials of the wave plates. In this case, they were quartz and MgF_2 because they are widely used as birefringent materials in polarimetry [28]. Specific information about their optical properties as refraction indices can be found in [24,29]. Due to the combinatorial nature of the problem, there are 2^N possible configurations of these two materials. In particular, the retarders presented in this work have been designed using $N = 5$ wave plates, which implies 32 possible configurations for each kind of retarder. Consequently, it is necessary to minimize the AcD for each configuration by means of the nine control variables. The large number of configurations (32) joined with the nine variables per setup requires a deep computational cost. Other setups with fewer numbers of wave plates were also considered, but the results cast a better fitting to the target with $N = 5$ wave plates. The more wave plates, the better results for the fitting, but it also increases the complexity of the problem.

3. NUMERICAL RESULTS AND DISCUSSION

To show the possibilities of this technique, three free-shaped retarders are designed by means of a combination of quartz and MgF_2 wave plates. The target retardation, $\Delta_0(\lambda)$, depends on the experiment; in this work, three target functions were chosen: two step functions, and a triangular function. These functions are very general and cover many experimental cases. The spectrum $g(\lambda)$ plays an important role as weight; it will try to enhance the fitting for the wavelength with higher intensity than in that with lower intensity. However, for some designs, it can be convenient $g(\lambda)$ as numerical weight unrelated to the spectrum. This is the case we will consider in our designs.

The first design is called called an up-step retarder, and consists of a step function with values (retardation) of 0° and 90° in intervals of [500,600] nm and [600,700] nm, respectively. The second step shape retarder is named down-step and shows a retardation of 180° and 90°, i.e., a behavior of $\lambda/2$ and $\lambda/4$ for spectral ranges of [500,600] nm and [600,700] nm, respectively. Finally, the last retarder presents the shape of a triangular sawtooth with a peak at 600 nm and retardation of 90°. The basis of the triangle starts at 500 nm and ends at 700 nm with a constant retardation of 0° at the ends and a linear behavior from 500 nm to 600 nm (positive slope) and from 600 nm to 700 nm (negative slope).

In the proposed designs, the weight has been chosen discretely, zero or one. Thus, $g(\lambda) = 1$ for those regions of Ω where the retardation of the system must fit the target retardation. In contrast, $g(\lambda) = 0$ for those wavelengths where the fitting is not of interest; it is out of the spectral ranges where the retarder is designed. Discontinuities or steep areas in the target retardation are the most susceptible to exhibiting a bad fitting because Eq. (2) is usually a continuous function. Fortunately, in our design of the step-shaped retarders, the region of interest is the flat region of the discontinuity. For this reason, we chose $g(\lambda) = 0$ in the discontinuity regions:

$$g(\lambda) = \begin{cases} 1 \text{ if } \lambda \in [500,\ 580]\ \mathrm{nm} \cup [620,\ 700]\ \mathrm{nm} \\ 0 \text{ if } \lambda \in (580,\ 620)\ \mathrm{nm} \end{cases}. \quad (12)$$

The minimization of the AcD metric was performed for 32 possible configurations to discriminate which one produces the best fitting to the target. The main drawback of designing step-shaped retarders is that the smallest value of the AcD might not be the best choice. This is due to the cliff splitting the spectral interval into two regions. It is critical to achieve a suitable fitting in both regions. For this reason, a new metric that allows discriminating the best configuration is introduced. A new metric called the peak distance is defined as the distance between the target retardation and the peak of the overall retardation in a spectral range, Ω:

$$\varepsilon = \max(\Delta - \Delta_0). \quad (13)$$

The weight function was set to zero in the cliff region to guarantee a good fitting on the bottom and top of the step; however, around the cliff area, the fitting remained bad in some cases.

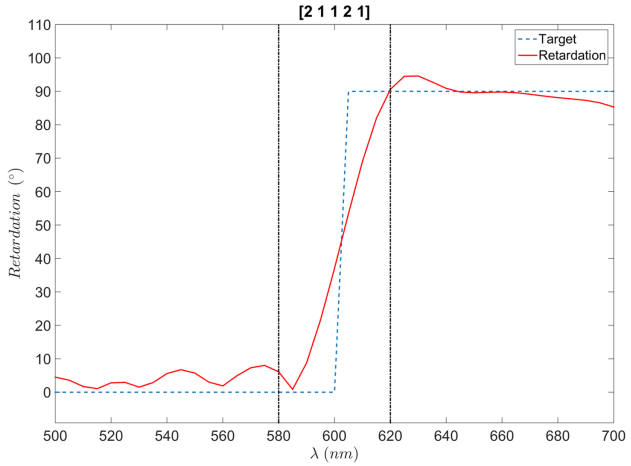

Fig. 2. Fit to up step for the configuration with $N = 5$ wave plates. "1" and "2" are quartz and MgF_2, respectively. The blue line is the target to achieve, and the red line is the retardation achieved with optimization. The area between the black lines is not taken into account.

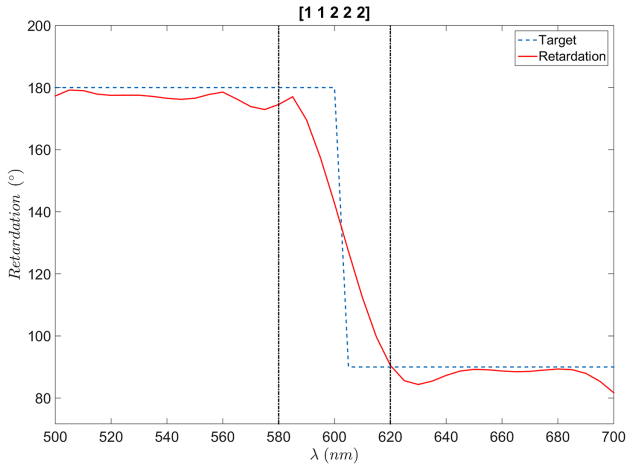

Fig. 3. Fit to down step for the configuration with $N = 5$ wave plates. "1" and "2" are quartz and MgF_2, respectively. (a) Between 90° and 0° and (b) between 180° and 90°. The blue line is the target to achieve, and the red line is the retardation achieved with optimization. The area between the black lines is not taken into account.

Accordingly, an extension of the cliff should be discarded. In our design, the regions of interest were $\Omega_1 = [500,\ 580]$ nm and $\Omega_2 = [620,\ 700]$ nm. The interval (580, 620) nm defines the extended cliff area and cannot be taken into account for applying the peak distance (areas between black lines in Figs. 2 and 3). Once the AcD is minimized, the peak distance is applied to determine the best configuration. In Figs. 2 and 3, the designed step retarders with the best optimized configurations in brackets are shown. For our analysis, we have labeled as "1" and "2" the quartz and MgF_2 wave plates, respectively.

In Table 1, the optimal thicknesses and azimuths that determine the behavior of the retarders are summarized along with the peak distances, ε_1 and ε_2, for their corresponding spectral intervals, Ω_1 and Ω_2. As we can see in Fig. 2, the achieved retardation in the spectral regions of interest is quite similar to the target. When the step is 180°–90°, Fig. 2, the best configuration

Table 1. Thicknesses, d_j, in Micrometers and Azimuths, ϕ_j, and Peak Distances, ε_j, in Degrees for Optimized Configurations

Retarder	Down Step	Up Step	Triangular
d_1 (μm)	291.0	227.2	139.5
d_2 (μm)	318.7	233.9	187.9
d_3 (μm)	112.2	202.0	27.2
d_4 (μm)	179.5	383.0	534.2
d_5 (μm)	293.0	234.5	302.7
ϕ_1 (°)	0	0	0
ϕ_2 (°)	128.2	54.6	58.9
ϕ_3 (°)	30.0	40.9	88.3
ϕ_4 (°)	10.6	124.7	152.7
ϕ_5 (°)	73.8	76.2	71.7
ε_1 (°)	7.08	8.01	–
ε_2 (°)	8.29	4.69	–
ε (°)	–	–	2.81

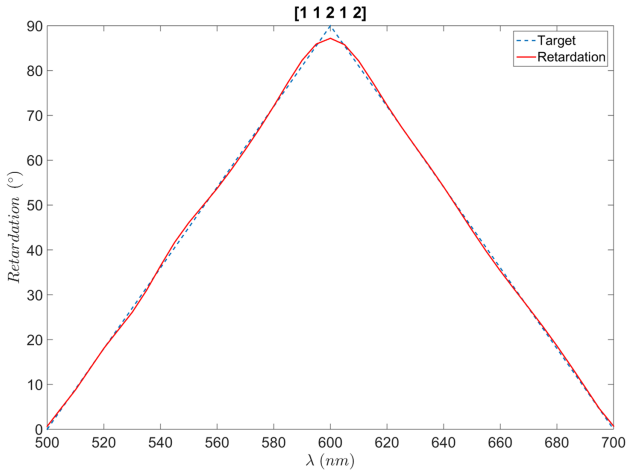

Fig. 4. Fit to triangular retardation for the configuration with $N = 4$ wave plates. "1" and "2" are quartz and MgF_2, respectively. The blue line is the target to achieve, and the red line is the retardation achieved with optimization.

with $N = 5$ wave plates is [11222] and the maximum errors in both spectral regions are $\varepsilon_1 = 7.08°$ and $\varepsilon_2 = 8.29°$. When the step is ascending, for instance, Fig. 3, where the step is 0°–90°, these good values of errors remain or decrease as in the second spectral region where $\varepsilon_2 = 4.69°$.

To test the method with other target shapes, we chose as a third studied case a triangular retarder. In this situation, the weight was defined as $g(\lambda) = 1$ for all λ in the spectral range of $\Omega = [500,\ 700]$ nm. The lack of discontinuities in the triangular shape justifies this election. A graphical representation of the best configuration for this retarder, [11212], can be seen in Fig. 4. Numerical results about thicknesses, azimuths, and ε are also shown in Table 1.

For this type of variable retardation, the obtained retardation fits better to the target one, i.e., the target and result are virtually the same except in the vertex where the error is $\varepsilon = 2.81°$. The stability under angular errors (orientation) and manufacturing tolerances in the wave plate thicknesses were also analyzed. Thus, denoting the optimal thicknesses and angles [See Table 1] by $\phi^0 = (0, \phi_2^0, \phi_3^0, \phi_4^0, \phi_5^0)$ and $d^0 = (0, d_2^0, d_3^0, d_4^0, d_5^0)$,

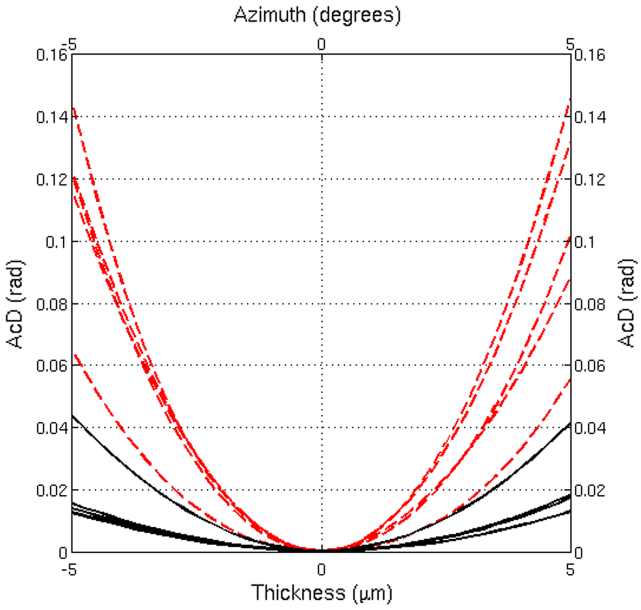

Fig. 5. Stability of AcD in the triangular retarder under small variations around the optimal thickness (continuous black) and thicknesses (red dashed).

respectively, the AcD is analyzed under small variations of each variable around the optimal value. If the angular stability is analyzed, the AcD is studied for each angular variable in the interval centered in the optimal solution $[\phi_i^0 - \zeta,\ \phi_i^0 + \zeta]$, where ζ is the interval radius with a length of 5°. The study of the thickness stability is analogous: the AcD is analyzed in the interval $[d_i^0 - \Lambda,\ d_i^0 + \Lambda]$, the radius in this case being $\Lambda = 5$ μm. In Fig. 5, the stability of the AcD for small variations around the optimal azimuths and thicknesses of the triangular retarder is shown. The results show a higher stability under errors in thickness than in the orientation of the wave plates. Similar plots with identical conclusions are obtained in the cases of up-step and down-step retarders; however, their representations have been omitted.

4. CONCLUSION

In this work, we present a technique to achieve free-shaped retarders in a broad spectral range using wave plates of different materials. For that, the thickness and the azimuth of each wave plate are optimized through a merit function that takes into account the entire system. As an example, numerical results have been presented for different target retardations, achieving errors of less than 10%. Moreover, the shown configurations present a high stability under small variations in their orientations and thicknesses.

Disclosures. The authors declare no conflicts of interest.

Data availability. Data underlying the results presented in this paper are not publicly available at this time but may be obtained from the authors upon reasonable request.

REFERENCES

1. D. H. Goldstein, *Polarized Light* (CRC Press, 2010).
2. D. Clarke and J. F. Grainger, *Polarized Light and Optical Measurement: International Series of Monographs in Natural Philosophy* (Elsevier, 2013), Vol. **35**.
3. D. S. Kliger and J. W. Lewis, *Polarized Light in Optics and Spectroscopy* (Elsevier, 2012).
4. J. Sambles, "Polarized light in optics and spectroscopy," J. Mod. Opt. **38**, 1204–1205 (1991).
5. J. J. Gil and R. Ossikovski, *Polarized Light and the Mueller Matrix Approach* (CRC Press, 2016).
6. R. King, "Quarter-wave retardation systems based on the Fresnel rhomb principle," J. Sci. Instrum. **43**, 617 (1966).
7. S. Pancharatnam, "Achromatic combinations of birefringent plates," in *Proceedings of the Indian Academy of Sciences-Section A* (Springer, 1955), Vol. **41**, pp. 137–144.
8. P. Hariharan, "Achromatic retarders using quartz and mica," Mea. Sci. Technol. **6**, 1078 (1995).
9. P. Hariharan, "Broad-band apochromatic retarders: choice of materials," Opt. Laser Technol. **34**, 509–511 (2002).
10. H. Kikuta, Y. Ohira, and K. Iwata, "Achromatic quarter-wave plates using the dispersion of form birefringence," Appl. Opt. **36**, 1566–1572 (1997).
11. D.-E. Yi, Y.-B. Yan, H.-T. Liu, and G.-F. Jin, "Broadband achromatic phase retarder by subwavelength grating," Opt. Commun. **227**, 49–55 (2003).
12. S. Shen, J. She, and T. Tao, "Optimal design of achromatic true zero-order waveplates using twisted nematic liquid crystal," J. Opt. Soc. Am. A **22**, 961–965 (2005).
13. Y.-J. Jen, M.-J. Lin, S.-K. Yu, and C.-C. Chen, "Extended broadband achromatic reflective-type waveplate," Opt. Lett. **37**, 4296–4298 (2012).
14. Y.-J. Jen, A. Lakhtakia, C.-W. Yu, C.-F. Lin, M.-J. Lin, S.-H. Wang, and J.-R. Lai, "Biologically inspired achromatic waveplates for visible light," Nat. Commun. **2**, 363 (2011).
15. J.-B. Masson and G. Gallot, "Terahertz achromatic quarter-wave plate," Opt. Lett. **31**, 265–267 (2006).
16. J. Ma, J.-S. Wang, C. Denker, and H.-M. Wang, "Optical design of multilayer achromatic waveplate by simulated annealing algorithm," Chin. J. Astron. Astrophys. **8**, 349 (2008).
17. Z. Chen, Y. Gong, H. Dong, T. Notake, and H. Minamide, "Terahertz achromatic quarter wave plate: design, fabrication, and characterization," Opt. Commun. **311**, 1–5 (2013).
18. P. Hariharan and P. Ciddor, "Broad-band superachromatic retarders and circular polarizers for the UV, visible and near infrared," J. Mod. Opt. **51**, 2315–2322 (2004).
19. M. Emam-Ismail, "Retardation calculation for achromatic and apochromatic quarter and half wave plates of gypsum based birefringent crystal," Opt. Commun. **283**, 4536–4540 (2010).
20. A. Saha, K. Bhattacharya, and A. K. Chakraborty, "Achromatic quarter-wave plate using crystalline quartz," Appl. Opt. **51**, 1976–1980 (2012).
21. J. L. Vilas and A. Lazarova-Lazarova, "A simple analytical method to obtain achromatic waveplate retarders," J. Opt. **19**, 045701 (2017).
22. J. M. Herrera-Fernandez, J. L. Vilas, L. M. Sanchez-Brea, and E. Bernabeu, "Design of superachromatic quarter-wave retarders in a broad spectral range," Appl. Opt. **54**, 9758–9762 (2015).
23. J. L. Vilas, L. M. Sanchez-Brea, and E. Bernabeu, "Optimal achromatic wave retarders using two birefringent wave plates," Appl. Opt. **52**, 1892–1896 (2013).
24. G. Ghosh, "Dispersion-equation coefficients for the refractive index and birefringence of calcite and quartz crystals," Opt. Commun. **163**, 95–102 (1999).
25. H. Hurwitz, Jr. and R. C. Jones, "A new calculus for the treatment of optical systems," J. Opt. Soc. Am. **31**, 493–495 (1941).
26. R. Barakat, "Jones matrix equivalence theorems for polarization theory," Eur. J. Phys. **19**, 209–216 (1998).
27. J. C. Lagarias, J. A. Reeds, M. H. Wright, and P. E. Wright, "Convergence properties of the Nelder–Mead simplex method in low dimensions," SIAM J. Optim. **9**, 112–147 (1998).
28. D. Clarke, *Stellar Polarimetry* (Wiley, 2009).
29. M. Bass, C. DeCusatis, J. Enoch, V. Lakshminarayanan, G. Li, C. MacDonald, V. Mahajan, and E. Van Stryland, *Handbook of Optics Volume IV: Optical Properties of Materials*, 3rd ed. (McGraw-Hill, 2009).